NANO LETTERS

2008
Vol. 8, No. 8
2351-2355

Electroluminescence from Single-Wall Carbon Nanotube Network Transistors

E. Adam,† C. M. Aguirre,† L. Marty,‡ B. C. St-Antoine,† F. Meunier,§ P. Desjardins,† D. Ménard,† and R. Martel*,‡

Regroupement Québécois sur les Matériaux de Pointe (RQMP), Département de Génie Physique, École Polytechnique de Montréal, Montréal QC H3C 3A7, Canada, Département de Chimie, Université de Montréal, Montréal QC H3T 1J4, Canada, et Département de Physique, Université de Montréal, Montréal QC H3T 1J4, Canada

Received April 25, 2008

ABSTRACT

The electroluminescence (EL) properties from single-wall carbon nanotube network field-effect transistors (NNFETs) and small bundle carbon nanotube field effect transistors (CNFETs) are studied using spectroscopy and imaging in the near-infrared (NIR). At room temperature, NNFETs produce broad (∼180 meV) and structured NIR spectra, while they are narrower (∼80 meV) for CNFETs. EL emission from NNFETs is located in the vicinity of the minority carrier injecting contact (drain) and the spectrum of the emission is red shifted with respect to the corresponding absorption spectrum. A phenomenological model based on a Fermi-Dirac distribution of carriers in the nanotube network reproduces the spectral features observed. This work supports bipolar (electron−hole) current recombination as the main mechanism of emission and highlights the drastic influence of carrier distribution on the optoelectronic properties of carbon nanotube films.

Single wall carbon nanotube (SWNT) devices have been shown to exhibit rich electro-optical effects. In particular, near-infrared (NIR) electroluminescence[1] (EL) and photoconductivity in nanotube transistors,[2] as well as photovoltaic effects in nanotube p-n junction diodes[3] have been demonstrated in devices in which the active region is made of individual carbon nanotubes. More recently, researchers have begun to investigate the properties of carbon nanotube networks for optoelectronic applications. It has been demonstrated that thin carbon nanotube sheets and carbon nanotube network transistors (NNFETs) made from these ensembles of nanostructures exhibit exciting properties such as photoconductivity[4] and bolometric response.[5] The electroluminescence properties of this new material, however, have not been investigated.

Experimental and theoretical studies on individual carbon nanotube transistors (CNFETs) revealed that EL from ambipolar devices involves the recombination of electron−hole pairs near a p-n junction that is electrostatically induced in the channel.[1,6–9] EL has also been observed in cases where no p-n junction is expected, such as in partially suspended CNFETs,[10,11] at fixed defect sites in ambipolar CNFETs,[12] and in unipolar CNFETs.[13] Alternative mechanisms involving either the impact excitation of hot carriers[10,14] or thermal emission[11] were proposed to explain these observations. Because of the presence of a statistical ensemble of individual nanotube emitters in a network, the investigation of EL from NNFETs should provide additional insights into the possible EL processes.

In this communication, we report on the EL properties of network transistors made from carbon nanotube sources having different diameter distributions. We compare the EL emission spectrum of these devices both to their corresponding absorption spectrum and to the emission spectrum of individual CNFETs emitters. Our analysis reveals that EL in these systems is dominated by emission from large diameter nanotubes instead of from the entire nanotube population. This feature is well-reproduced by a phenomenological model based on the Fermi-Dirac distribution of carriers in the nanotube network. Moreover, our spatial imaging results reveal localized EL at the minority carrier injection contact and show that the dominant EL pathway in unipolar NNFETs involves the recombination of bipolar (electron−hole) current. Hence, impact excitation and thermal emission can be ruled out as explanations for the origin of the observed EL in our network devices.

Light emitting carbon nanotube transistors were fabricated using three different SWNT sources. The first consists in nanotubes synthesized using a laser ablation method[15] (LA nanotubes), while the other two were produced by chemical vapor deposition methods using either a high pressure process[16] (HiPco nanotubes) or Co−Mo catalysts[17] (Co-

* Corresponding author. E-mail: r.martel@umontreal.ca.
† Département de Génie physique, École Polytechnique de Montréal.
‡ Département de Chimie, Université de Montréal.
§ Département de Physique, Université de Montréal.

10.1021/nl8011825 CCC: $40.75
Published on Web 07/04/2008

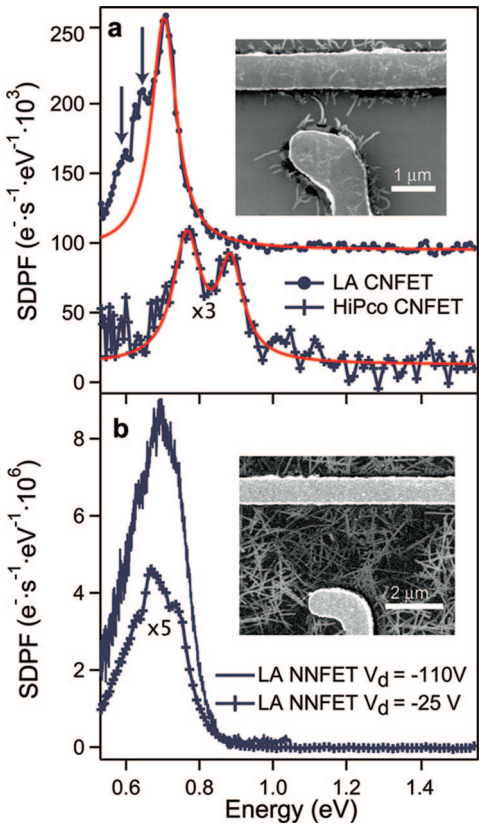

Figure 1. SDPF: Spectral detected photon flow. (a) Typical EL spectra of LA CNFET (top) and HiPco CNFET (bottom) acquired using an exposure time (t_{exp}) of 2 min. The electrode spacing is 1 μm. The LA spectrum is from a CNFET operating at $V_d = -5$ V, $V_g = -2.5$ V, while the HiPco spectrum is from a device operating at $V_d = -9.5$ V, $V_g = -20$ V. Lorentzian fits are also shown and give line widths of ~80 meV for CNFETs. For clarity, LA CNFET spectrum has been upshifted by 100 units along the vertical axis. (b) Typical near-infrared EL spectra from a LA NNFET biased at $V_d = -25$ V (bottom curve) and $V_d = -110$ V (top curve) at $V_g = -20$ V with $t_{exp} = 2$ min. The electrode spacing is 3 μm. Insets: SEM images of the devices.

MoCAT nanotubes). The significantly larger diameters of LA nanotubes (1.1−1.5 nm) compared with those contained in CoMoCAT (0.6−1.1 nm) and HiPco (0.7−1.1 nm) sources are a central feature of this study.

In order to establish a solid reference base, we measured EL emission from both individual bundle CNFETs and NNFETs. Measurements on both were essential since there have only been a limited number of reports on the EL spectral characteristics of individual carbon nanotube emitters.[10,11,13,18] Individual CNFETs are made from a small individual bundle of either HiPco and LA nanotubes, while NNFETs are fabricated from networks of LA and CoMoCAT nanotubes. The insets in Figure 1a,b show SEM images representative of CNFET and NNFET devices. CNFET channels consist mainly of an individual SWNT bundle while the channel of the NNFETs consists of a submonolayer network of interconnected SWNTs. All measured transistors displayed p-type semiconducting electrical characteristics in air. However, it was possible to convert the devices from unipolar to ambipolar by covering them with a 150 nm parylene-C coating followed by an annealing in vacuum at 200 °C for 24 h, a procedure similar to what has been previously reported.[19]

EL spectra were acquired at room temperature using the Montreal infrared spectrometer (SIMON), a state-of-the-art NIR spectrometer/imager designed for the Mont-Megantic astronomical telescope (OMM, Quebec, Canada).[20] Supporting Information provides further details concerning device fabrication as well as electrical and EL measurement protocols.

Examples of EL spectra from CNFETs fabricated using LA and HiPco sources are shown in Figure 1a. The transistors were biased in order to obtain the same value of source−drain currents ($I_{ds} = 5.5$ μA) while allowing for sufficiently high emission signal to acquire the spectra. The EL characteristics of the CNFET fabricated using the LA source (top curve) were measured with gate (V_g) and drain (V_d) bias voltages of −2.5 V and −5 V, respectively. An electroluminescence efficiency (total emitted photons per injected carrier) of approximately $\eta_e \sim 10^{-6}$ was measured in these conditions. A narrow peak centered at 0.70 eV having a Lorentzian line width of ~80 meV is clearly resolved. We also observe two satellite peaks (see arrows) red shifted by 60 and 110 meV of the main EL feature. The bottom curve in Figure 1a presents the emission spectrum for a HiPco device biased at $V_d = -9.5$ V and $V_g = -20$ V. This spectrum shows two narrow peaks emitting at energies of 0.77 and 0.89 eV. The higher emission energies measured for this bundle are consistent with the smaller diameters of the nanotubes contained in the HiPco source used to fabricate the device. Lorentzian line fits to these peaks resulted in line widths that were essentially identical to those corresponding to the LA device (~80 meV).

Spectra acquired on a number of CNFETs consistently exhibited emission peaks having ~80 meV line widths leading us to assert that each peak corresponds to the emission originating from an individual carbon nanotube. More than one peak can be resolved for bundles of HiPco nanotubes because the larger spread in energies associated to these smaller diameter nanotubes reduces the overlap between the emission from distinct nanotubes. The satellite peaks observed in the EL spectra from LA devices can be attributed to simultaneously emitting nanotubes; we hypothesize, however, that they may also result from the emission of dark excitons,[21] biexcitons,[22] or localized excitons.[23] The lower signal-to-noise ratio of the EL from HiPco devices did not allow us to confirm the presence of these fine structures.

Figure 1b presents typical spectra of LA-NNFETs. The bottom curve shows the results for a device biased at $V_g = -20$ V and $V_d = -25$ V with $I_{ds} = 9$ μA. The EL efficiency is an order of magnitude higher than that of the CNFET devices, $\eta_e \sim 10^{-5}$. The emission from LA-NNFETs is centered at 0.69 eV (essentially the same value as for the CNFET from the same nanotube source), but in contrast to CNFETs, the peak is much broader (~180 meV). To confirm the presence of spectral fine structure, measurements were also taken by biasing the device at $V_d = -110$ V (top curve) in order to operate the SIMON spectrometer in its maximum

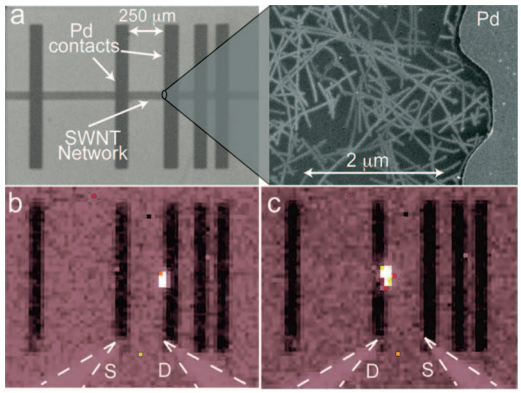

Figure 2. (a) SEM images of a long channel NNFET made from LA nanotubes. The electrode spacing is 250 μm and the width of the SWNT network is 100 μm. (b) NIR images of the EL in a typical long channel unipolar NNFET. The light emission zone is located at the drain (D) contact region at $V_g = V_d/2 = -30$ V and $V_d = -60$ V. (c) The emission zone changes side when the voltage polarity is reversed, i.e., $V_g = 30$ V and $V_d = 60$ V.

resolving power mode (see Supporting Information). Except for an increase in the light intensity, the broad EL line shape was found to be independent of the biasing conditions and is characteristic of all NNFETs fabricated using the LA nanotube source.

These results allow us to highlight a number of important observations regarding the EL emission from NNFETs. First, the energy range (0.60−0.85 eV) and fine structure observed in the EL spectrum of LA nanotubes is similar to their corresponding PL spectrum (see Supporting Information), which is consistent with the diameter distribution of the LA source. This finding strongly suggests that the radiative recombination of excitons that is responsible for the PL signal[24] is the same process leading to EL in carbon nanotube networks. Second, the broad line shape of the EL emission indicates that a large population of nanotubes is participating to the EL signal. Thus, the EL emission appears to be a superposition of several narrow peaks originating from individual carbon nanotube emitters.

The spatial resolution of the SIMON spectrometer/imager (∼30 μm/pixel) allowed us to further investigate the origin of EL in NNFETs. Long channel unipolar p-type NNFETs ($L = 250$ μm, $W = 100$ μm), as the one pictured in Figure 2a, were used for these experiments. The device was biased at both negative (Figure 2b) and positive voltages (Figure 2c) in order to invert the location of the source and drain electrodes. As evidenced from these images, the NIR emission always occurred in the vicinity of the minority carrier injecting contact (drain electrode).

If impact excitation were the mechanism responsible for the EL signal, the maximum of the emission should occur at the source, where hot majority carriers are injected.[13] Alternatively, if Joule heating were at the origin of the EL in NNFETs, the emission spot would be located along the channel and should be more intense in the middle.[11] Hence, we can rule out impact excitation and thermal emission as mechanisms responsible for the EL emission in our devices.

The position of the emission spot rather suggests that radiative excitonic recombination takes place when minority carriers (here electrons) leak from the drain to interact with majority carriers (holes). The fact that no electron current is measured in the electrical characteristics (exclusive p-type behavior) suggests that the leakage is a dynamic effect due to a modification of the band-bending conditions near the drain contact. That is, under high current unipolar operation, holes may be backscattered and accumulated at the drain. This generates enough positive space charge near the contact to pull the bands down and promote electron tunneling across the Schottky barrier. This mechanism has been previously suggested to account for the enhanced EL emission intensity near the contacts in ambipolar CNFETs operated at high bias.[6,12]

Furthermore, if bipolar current recombination is indeed at the origin of EL in unipolar NNFET, the intensity of the emission will be limited by the tunneling rate of minority carriers. As discussed above, this rate depends on the number of positive space charge accumulated at the drain. Thus, the emission rate should increase as the total hole current across the device increases. We verified that this was in fact the case. Moreover, unipolar devices that had been converted to ambipolar devices using the procedure outlined above, displayed identical EL emission line shapes and localized contact emission. This finding further suggests that excitonic recombination of electrons and holes, injected from opposite contacts, is the main mechanism responsible for EL in NNFET.

It is well-established that the optical absorption spectrum of a bulk nanotube sample is a superposition of narrow peaks, each corresponding to an optical transition of a given nanotube species.[24] Thus, the population of carbon nanotubes contributing to the EL signal can be extracted by comparing the EL emission spectra with the absorption spectra of a network from the same nanotube source. The normalized optical absorption spectrum of thick networks (∼300 nm) of LA (dotted curve) and CoMoCAT (bold curve) nanotubes deposited on glass substrates are shown in Figure 3a. The energy ranges for the first optical transitions (E_{11}^S) of LA (0.60−0.85 eV) and CoMoCAT (0.70−1.50 eV) nanotubes are direct signatures of their significantly different diameter distributions (1.1−1.5 nm for LA and 0.6−1.1 nm for CoMoCAT nanotubes). Moreover, because only a few specific nanotube helicities [$(n,m) = (6,5)$, (7,5), (8,4), (8,3), (7,6)] dominate the diameter distribution of CoMoCAT nanotubes, distinct peaks at ∼1.05 and 1.2 eV appear in the absorption spectra.[25]

Figure 3b depicts typical EL spectra from unipolar p-type NNFETs fabricated using both LA (circles) and CoMoCAT (crosses) nanotube networks. The broad emission line width in both cases (∼180 meV) compared with typical line width for CNFETs (∼80 meV) indicates that many carbon nanotube emitters participate to the EL signal. Moreover, the emission peak for the CoMoCAT device is centered at higher energy (0.80 eV) compared with that for LA networks (0.70 eV), which is consistent with the smaller overall diameters of nanotubes present in the CoMoCAT distribution. In both cases, however, the EL maximum appears at lower energies than does the maximum of the absorption peak. The EL

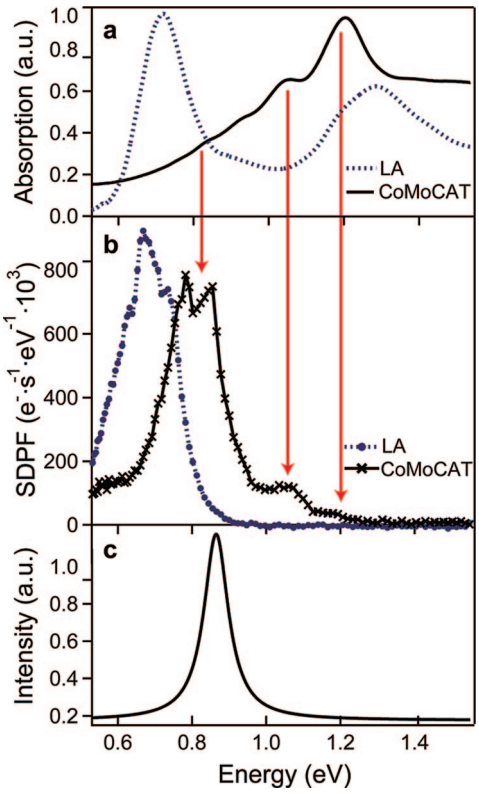

Figure 3. (a) Absorption spectra recorded from networks made with CoMoCAT and LA sources. (b) Corresponding EL spectra obtained using SIMON with the Amici prism. The spectra were acquired for $t_{exp} = 2$ min using $V_d = -25$ V, $V_g = -20$ V and $V_d = -55$ V, $V_g = -20$ V for the LA and CoMoCAT spectra, respectively. The electrode spacing is 3 μm for the LA NNFET and 1 μm for the CoMoCAT NNFET. (c) Simulated EL spectrum for the CoMoCAT source.

signal is red shifted by 25 meV for LA nanotube networks. The shift is most significant for the CoMoCAT nanotubes where the peaks appearing in the absorption spectra (1.2 and 1.05 eV) are very weak in the EL signal (see arrows). The EL maximum of CoMoCAT NNFETs is offset by 400 meV with respect to the absorption maximum.

These offsets are too large to be accounted for by the Stokes shift alone (only few millielectronvolts).[24] Moreover, a red shift due to a change in dielectric constant is also unlikely given that the absorption characteristics were measured for networks deposited in similar dielectric environments (thermal oxide layer on silicon substrate and microscope glass slide). These results show that only a subset of the entire nanotube population contributes to the main EL signal. The lower emission energy reveals that large diameter carbon nanotubes contribute the most to the EL spectra.

Two different effects can account for the emission being dominated by large diameter nanotubes: (i) the carrier density distribution is higher on large diameter nanotubes and (ii) an energy transfer process takes place from small to large diameter nanotubes. We investigated the first mechanism by calculating the carrier density distribution in the network. We assumed that the carriers are relaxed throughout the network (carrier relaxation time $\ll$ carrier recombination time). Briefly, we evaluated the carrier density for each nanotube in the network by integrating, over energy, the product of the room temperature Fermi-Dirac distribution by the one-dimensional (1D) density of states. The emission for each possible nanotube helicity in the network was simulated by a Lorentzian having a line width of 80 meV and an amplitude corresponding to the square of the calculated carrier density. The square was taken in order to account for the recombination process (EL intensity is proportional to the product of electrons and holes). Finally, the simulated EL spectrum of the network is simply obtained by the sum of the Lorentzians of the individual nanotubes weighted by their relative population in the distribution. The relative population of each nanotube species was extracted from the analysis of the absorption spectrum (see Supporting Information). The simulated emission spectrum for the CoMoCAT network spectrum (Figure 3c) is located at 0.87 meV and displays a line width of 80 meV.

A comparison with the CoMoCAT emission data shows that the model reproduces remarkably well the spectral shift observed experimentally. The simulated EL spectrum is found to be completely dominated by SWNTs having 1.1 nm diameters, although they correspond to only 4% of the total population. The intensity of the EL emission from small diameter nanotubes is negligible due to the Fermi-Dirac and band edge distributions of these SWNTs. Hence, the carrier distribution in networks drastically influences the population of exciton states that are formed. The fact that the experimental EL spectra measured is somewhat broader and at lower energies is most likely due to the poor estimate of the relative population of large carbon nanotubes used in our calculations (see Supporting Information). However, the weak experimental peaks observed at higher energies (1.05 and 1.2 eV) are not reproduced by our model, possibly because of the nonequilibrium condition at high voltage.

Recent photoabsorption and photoluminescence studies have highlighted the importance of carrier migration and Förster type energy transfer mechanisms in surfactant/polymer encapsulated carbon nanotube bundles.[26–28] While carrier migration is somehow consistent with our model, there was no need to incorporate Förster energy transfer in the present study.

In summary, we have shown that NNFETs are electroluminescent devices having broad and tunable EL spectra. The spectral line width and the specific emission wavelength mainly depend on the population of the largest SWNTs within a source. This remarkably strong effect appears to be a property of networks and should not be observed for individual CNFETs. From a practical point of view, in order to achieve carbon nanotube network devices displaying an emission tunability that covers the full near-infrared range that is available to SWNTs, an effective enrichment and separation of semiconducting nanotubes on the basis of their diameter will be essential.

Acknowledgment. The authors thank M. Paillet, D. McGuire, M. Côté, C. Silva, and B. Movaghar for valuable discussions, L. Albert, R. Doyon, and P. Vallée for technical assistance and access to SIMON, and M. Trudel, J. Crochet, and R. Leonelli for the PL measurements. We are grateful to B. Simard and

D. E. Resasco for the generous donation of the LA and CoMoCAT nanotubes, respectively. This project is supported by the Canada Research Chair (CRC), NSERC, and FQRNT programs.

Supporting Information Available: Description of device fabrication, optical set-ups, electrical characteristics of ambipolar NNFETs, EL spectrum evolution with voltages, photoluminescence spectrum of LA source, Raman characterization, and details on the simulation of EL in NNFETs. This material is available free of charge via the Internet at http://pubs.acs.org.

References

(1) Misewich, J. A.; Martel, R.; Avouris, Ph.; Tsang, J. C.; Heinze, S.; Tersoff, J. *Science* **2003**, *300*, 783–786.
(2) Freitag, M.; Martin, Y.; Misewich, J. A.; Martel, R.; Avouris, Ph. *Nano Lett.* **2003**, *3*, 1067–1071.
(3) Lee, J. U. *Appl. Phys. Lett.* **2005**, *87*, 073101–3.
(4) Fujiwara, A.; Matsuoka, Y.; Suematsu, H.; Ogawa, N.; Miyano, K.; Kataura, H.; Maniwa, Y.; Suzuki, S.; Achiba, Y. *Jpn. J. Appl. Phys.* **2001**, *40*, L1229–L1231.
(5) Itkis, M. E.; Borondics, F.; Yu, A.; Haddon, R. C. *Science* **2006**, *312*, 413–416.
(6) Freitag, M.; Chen, J.; Tersoff, J.; Tsang, J. C.; Fu, Q.; Liu, J.; Avouris, Ph. *Phys. Rev. Lett.* **2004**, *93*, 076803.
(7) Guo, J.; Alam, M. A. *Appl. Phys. Lett.* **2005**, *86*, 023105–3.
(8) Tersoff, J.; Freitag, M.; Tsang, J. C.; Avouris, Ph. *Appl. Phys. Lett.* **2005**, *86*, 263108–3.
(9) McGuire, D. L.; Pulfrey, D. L. *Nanotechnology* **2006**, *17*, 5805–5811.
(10) Chen, J.; Perebeinos, V.; Freitag, M.; Tsang, J.; Fu, Q.; Liu, J.; Avouris, Ph. *Science* **2005**, *310*, 1171–1174.
(11) Mann, D.; Kato, Y. K.; Kinkhabwala, A.; Pop, E.; Cao, J.; Wang, X.; Zhang, L.; Wang, Q.; Guo, J.; Dai, H. *Nature Nanotech.* **2007**, *2*, 33–38.
(12) Freitag, M.; Tsang, J. C.; Kirtley, J.; Carlsen, A.; Chen, J.; Troeman, A.; Hilgenkamp, H.; Avouris, Ph. *Nano Lett.* **2006**, *6*, 1425–1433.
(13) Marty, L.; Adam, E.; Albert, L.; Doyon, R.; Ménard, D.; Martel, R. *Phys. Rev. Lett.* **2006**, *96*, 136803–4.
(14) Perebeinos, V.; Avouris, Ph. *Phys. Rev. B* **2006**, *74*, 121410–4.
(15) Kingston, C. T.; Jakubek, Z. J.; Dénommée, S.; Simard, B. *Carbon* **2004**, *42*, 1657–1664.
(16) Bronikowski, M. J.; Willis, P. A.; Colbert, D. T.; Smith, K. A.; Smalley, R. E. *J. Vac. Sci. Technol. A* **2001**, *19*, 1800–1805.
(17) Kitiyanan, B.; Alvarez, W. E.; Harwell, J. H.; Resasco, D. E. *Chem. Phys. Lett.* **2000**, *317*, 497–503.
(18) Freitag, M.; Perebeinos, V.; Chen, J.; Stein, A.; Tsang, J. C.; Misewich, J. A.; Martel, R.; Avouris, Ph. *Nano Lett.* **2004**, *4*, 1063–1066.
(19) Martel, R.; Derycke, V.; Lavoie, C.; Appenzeller, J.; Chan, K. K.; Tersoff, J.; Avouris, Ph. *Phys. Rev. Lett.* **2001**, *87*, 256805.
(20) Albert, L. Ph. D., University de Montréal, 2006.
(21) Kiowski, O.; Arnold, K.; Lebedkin, S.; Hennrich, F.; Kappes, M. M. *Phys. Rev. Lett.* **2007**, *99*, 237402–4.
(22) Pedersen, T. G.; Pedersen, K.; Cornean, H. D.; Duclos, P. *Nano Lett.* **2005**, *5*, 291–294.
(23) Hartschuh, A.; Qian, H.; Meixner, A. J.; Anderson, N.; Novotny, L. *Nano Lett.* **2005**, *5*, 2310–2313.
(24) O'Connell, M. J.; Bachilo, S. M.; Huffman, C. B.; Moore, V. C.; Strano, M. S.; Haroz, E. H.; Rialon, K. L.; Boul, P. J.; Noon, W. H.; Kittrell, C.; Ma, J.; Hauge, R. H.; Weisman, R. B.; Smalley, R. E. *Science* **2002**, *297*, 593–596.
(25) Bachilo, S. M.; Balzano, L.; Herrera, J. E.; Pompeo, F.; Resasco, D. E.; Weisman, R. B. *J. Am. Chem. Soc.* **2003**, *125*, 11186–11187.
(26) Torrens, O. N.; Milkie, D. E.; Zheng, M.; Kikkawa, J. M. *Nano Lett.* **2006**, *6*, 2864–2867.
(27) Tan, P. H.; Rozhin, A. G.; Hasan, T.; Hu, P.; Scardaci, V.; Milne, W. I.; Ferrari, A. C. *Phys. Rev. Lett.* **2007**, *99*, 137402–4.
(28) Gadermaier, C.; Menna, E.; Meneghetti, M.; Kennedy, W. J.; Vardeny, Z. V.; Lanzani, G. *Nano Lett.* **2006**, *6*, 301–305.

NL8011825